Available online at www.sciencedirect.com

ScienceDirect

Biochemical and Biophysical Research Communications 351 (2006) 159–164

BBRC

www.elsevier.com/locate/ybbrc

Torsion of the central pair microtubules in eukaryotic flagella due to bending-driven lateral buckling

C. Li, C.Q. Ru *, A. Mioduchowski

Department of Mechanical Engineering, University of Alberta, Edmonton, Canada T6G 2G8

Received 7 September 2006
Available online 20 October 2006

Abstract

Inspired by recent interest in torsion of the central pair microtubules in eukaryotic flagella, a novel thin-walled elastic beam model is suggested to study critical condition under which uniform bending of a flagellum will cause lateral/torsional buckling of the central pair. The model is directed to the central pair itself and the role of all surrounding cross-linkings inside the flagellum is modeled as an equivalent surrounding elastic medium. The model predicts that bending-driven torsion of the central pair does occur when the radius of curvature of the bent flagellum reduces to a moderate critical value typically of tens of microns. In particular, this critical value is almost independent of the flagellum length, and more sensitive to the parameters defining the surrounding elastic medium than the shear modulus of microtubules. The predicted wavelengths of the torsional buckling mode are insensitive to the flagellum length and comparable to some known related experimental data. These results indicate that torsion of the central pair microtubules in flagella is inevitable as a result of bending-driven lateral buckling. This offers an entirely new insight into the ongoing research on the mechanism of the central pair torsion.

Keywords: Cell mechanics; Central pair; Microtubule; Flagella; Torsion; Lateral buckling

Cells can move with respect to their environment such as a fluid medium. A common propulsion mechanism for cell movement employs flagella (Latin plural for whip) [1–5]. Flagella are long whip-like organelles extending from the cell's body, and have a typical length of about 10 μ, although examples of ten times of this length are known. A cell typically has one or two flagella, which are encased into the cell's membrane so that the interior of a flagellum is accessible to the cell's cytoplasm. Flagella are motile and wiggle to move the cell. Some cells bend their flagella to produce a wavelike motion, whereas others rotate them in a manner similar to a ship's propeller. Torque and thrust generated by flagella can propel a cell at up to a few tens of microns per second [1–5].

In spite of a wide variety of eukaryotic cells, eukaryotic flagella consist of a unique common core structure, called "9 + 2" axoneme, that is about 200 nm in diameter [1,2] and contains nine outer doublet microtubules, equally spaced in a circle, and two bridged central pair of microtubules apart by a small distance of a few nanometers [1–5], as shown in Fig. 1. Each of the outer doublets is made up of a complete microtubule (called "A tubule") clutched by another incomplete microtubule (called "B tubule"), while the central pair microtubules are both complete. Extending from the outer doublets are sets of motor protein (called "dynein" arms) and nexin links that provide circumferential bridge to hold outer doublets together, and projecting inward are radial spokes that connect with a sheath enclosing the central pair microtubules. Here, it should be mentioned that structurally similar to flagella are cilia (Latin plural for eyelash), although cilia are much shorter than flagella in length and can be so numerous to cover the entire surface of a cell and wave like tall grass in the wind, creating currents in its fluid environment [1–5]. In addition to their obvious role in cellular motility, the flagellum and

---

* Corresponding author. Fax: +1 780 492 2200.
E-mail address: c.ru@ualberta.ca (C.Q. Ru).

0006-291X/$ - see front matter © 2006 Elsevier Inc. All rights reserved.
doi:10.1016/j.bbrc.2006.10.019

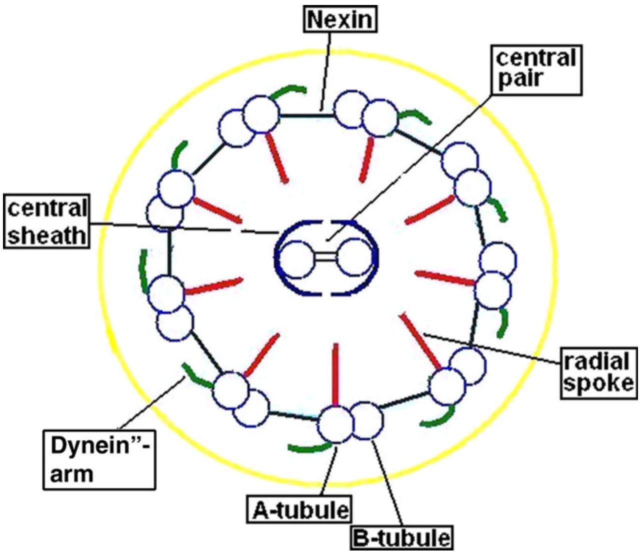

Fig. 1. The "9 + 2" axoneme of flagella and cilia.

cilium are believed to be also vital organelles in sensation and signal transduction across a wide variety of cell types.

Mechanical behavior of flagella, especially rod-like bending deformation of flagella and their hydrodynamic interaction with a surrounding fluid medium, is crucial for their biological functions. It is now widely accepted that bending and motility of flagella are generated by the dynein-driven sliding between doublet microtubules [1,2]. So, sliding-bending mechanics of flagella [6–13], and related hydrodynamics of flagella in a fluid medium [4,14–20] have been the focus of numerous earlier and recent experimental and theoretical researches. More recently, a relevant issue which has attracted considerable attention is bending-driven torsion of the central pair microtubules with respect to the outer doublets [21–28]. The exact mechanism and functions of torsion of the central pair are not yet fully understood. Since the central pair is believed to play a vital role in regulation of flagella motion [29,30], it is relevant to study the mechanism responsible for torsion of the central pair microtubules in eukaryotic flagella.

Inspired by the structural characteristics of the central pair, and the similarity between bending-induced torsion of the central pair and the lateral/torsional buckling of thin-walled elastic beams under bending [31–34], the present paper aims to study whether or not a reasonable bending of a flagellum could cause lateral/torsional buckling of the central pair. This problem is interesting especially in view of the fact that the central pair, as modeled as a single elastic beam, has a lower torsional rigidity. The justifications and details of the suggested elastic beam model will be given in second section. The model is used in third section to examine the critical bending and the wavelength of torsional buckling mode when the flagellum is bent in the principal plane of the central pair's cross-section of the maximum bending rigidity. Finally, the results obtained are summarized in fourth section. As will be seen below, for the first time in the literature, the present model shows that torsion of the central pair will occur inevitably, as a result of bending-driven lateral buckling, when a flagellum is bent and the bending exceeds a moderate critical value.

Basic parameters of the central pair and the surrounding elastic medium

The central pair of flagella is composed of two complete single microtubules, as shown in Fig. 1, surrounded by associated links and organelles. The present study focuses on structural behavior of the central pair itself, and the effects of all surrounding links and organelles inside the flagellum will be modeled approximately by an equivalent surrounding elastic medium, defined by two spring constants for transverse deflections of the central pair and one spring constant for torsion of the cross-section of the central pair.

As a whole, the central pair of microtubules, including the bridge linking the two microtubules, will be described as a single elastic beam of thin-walled cross-section. Assume that the two microtubules of the central pair are initially parallel to each other. Thus, the coordinate system is centered at the centroid of the central pair's cross-section, as shown in Fig. 2, where the x-axis is along the axial direction of the flagellum, and the y- and z-axes are along two mutually perpendicular principal directions of the cross-section, of maximum and minimum bending rigidities, respectively.

Let us now calculate bending rigidities EI_{yy} and EI_{zz} ($I_{yz} = 0$ due to the symmetry of the cross-section), where E is the longitudinal elastic modulus of microtubules [35–40]. Following the literature, the cross-section of a single microtubule will be treated as an equivalent circular annular shape, with an equivalent thickness $h \approx 3$ nm (see e.g., [37,39]). Thus, all moments of inertia of the cross-section are defined based on such a thickness $h \approx 3$ nm. In addition, because the bridging linking the two microtubules has a much lower elastic modulus than the longitudinal modulus E, the contribution of the bridging to bending rigidities can be neglected. Thus, $EI_{zz} = 2E\frac{\pi(R_o^4-R_i^4)}{4} \approx 5.60 \times 10^{-23}$ N m^2, where, we have assumed

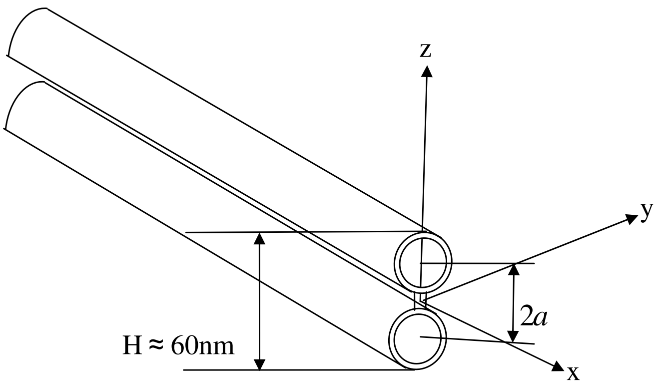

Fig. 2. The central pair microtubules modeled as a single elastic beam.

that the medium radius r_m of a single microtubule is 11.5 nm, and the outer radius $R_0 = 13$ nm and the inner radius $R_i = 10$ nm. Similarly, because the distance between the centers of the two microtubules is $2a \approx 34$ nm [9] (see Fig. 2), the bending rigidity EI_{yy} is obtained by the parallel-axis formula, which gives

$$EI_{yy} = 2E\left[\frac{\pi(R_o^4 - R_i^4)}{4} + \pi(R_o^2 - R_i^2)a^2\right] \approx 3.0 \times 10^{-22}\ \text{N m}^2.$$

On the other hand, torsional rigidity of the central pair, GJ, is proportional to shear modulus G of microtubules [41,42]. Because shear modulus G is more than two orders of magnitude lower than the longitudinal Young's modulus E, it is expected that microtubules and the central pair have lower torsional rigidities. In particular, the actual value of G is unknown in the literature. Here, following [43,44], we assume that G is about 10^4–10^6 Pa or $G/E = 10^{-5}$–10^{-3}. Thus neglecting the contribution of the bridging to torsional rigidity, torsional rigidity of the central pair will be given roughly by twice the torsional rigidity of a single microtubule. Thus, $GJ = 2GJ_o = 2G\frac{\pi(R_o^4 - R_i^4)}{2}$, where G is the shear modulus of microtubules [41,42] and J_o is the torsional constant of a single microtubule. Thus, taking $E = 1.9$ GPa [44], the values of EI_{yy} and EI_{zz}, and the range of the torsional rigidity GJ are given in Table 1.

The central pair is surrounded by mixed cytoplasm fluid and flagellar links. The modulus of cytoplasm fluid is around 10^2–10^5 Pa [45], while the moduli of flagellar links are around 10^4–10^6 Pa [35]. Therefore, the equivalent modulus E_0 of the surrounding elastic medium can be bounded reasonably by $10^3 < E_0 < 10^6$ Pa. Furthermore, because the ratio of the wavelength to the diameter of the central pair is about between 1 and 500, it is expected (see Fig. 1 of [46] or [47]) that the spring constant K_y, defined by the reaction force (per unit axial length of the central pair) against the deflection of the central pair in the y-direction, can be estimated by $K_y = (10^{-2}$–$1)E_0$. In addition, the spring constant K_y can be assumed to be approximately twice K_z, then $K_z = 0.5K_y$. Finally, because the distance between the centers of the two microtubules is about $2a = 34$ nm, simple calculation shows that the spring constant K_ϕ, defined by the reaction moment against the rotation of the central pair, can be given approximately by $K_\phi = 2K_ya^2$. The values of all these parameters, used in the present paper for the surrounding elastic medium, are summarized in Table 1.

Table 1
Parameters used in the present paper for the cross-section of the central pair and the equivalent surrounding elastic medium

Parameters	Value	Reference
r_m	11.5 nm	[9]
a	17 nm	[9]
E	1.9 GPa	[44], present paper
E_0	10^3–10^6 Pa	[35,45], present paper
K_y	$(10^{-2}$–$1)E_0$	[46], present paper
K_z	$0.5K_y$	Present paper
K_ϕ	$2K_ya^2$	Present paper
G/E	10^{-5}–10^{-3}	[43,44], present paper
EI_{yy}	3.00×10^{-22} N m^2	Present paper
EI_{zz}	5.60×10^{-23} N m^2	Present paper
GJ	10^{-27}–10^{-25} N m^2	Present paper
h	3 nm	[37,39], present paper
H	60 nm	[9]

Lateral buckling of the central pair bent in the plane of maximum bending rigidity

First, let us consider torsional/lateral buckling of the central pair when the flagellum is uniformly bent in the x–z plane. Under such a uniform bending, the pre-buckling deflection of the central pair, $w_0\,(x)$, is a quadratic function of x and thus $EI_{yy}w_0''(x)$ is a constant equal to the moment M_{yy} acting on the central pair prior to buckling ($M_{yy} = EI_{yy}w_0''(x)$). Let that y-directional buckling deflection of the central pair be $v(x)$, and buckling torsion of the cross-section of the central pair about the x-axis be $\phi\,(x)$. Thus, the reaction force and torque, acting on the central pair due to the surroundings, are $K_yv(x)$ and $K_\phi\phi(x)$, respectively, and lateral buckling of the central pair under the uniform bending M_{yy} is governed by [31–34]

$$EI_{zz}\frac{\mathrm{d}^4v(x)}{\mathrm{d}x^4} - M_{yy}\frac{\mathrm{d}^2\phi(x)}{\mathrm{d}x^2} + K_yv(x) = 0 \tag{1}$$

$$-GJ\frac{\mathrm{d}^2\phi(x)}{\mathrm{d}x^2} - M_{yy}\frac{\mathrm{d}^2v(x)}{\mathrm{d}x^2} + K_\phi\phi(x) = 0 \tag{2}$$

Assume that the central pair is hinged at its two ends and thus

$$v(x) = A\sin\frac{m\pi x}{L}, \quad \phi(x) = B\sin\frac{m\pi x}{L} \tag{3}$$

where L is the length of the flagellum, A and B are two real numbers, and integer m is the half-wave number of buckling mode. Thus, substituting (3) into (1, 2) gives

$$A\left[EI_{zz}\left(\frac{m\pi}{L}\right)^4 + K_y\right] = M_{yy}(-B)\left(\frac{m\pi}{L}\right)^2 \tag{4}$$

$$B\left[GJ\left(\frac{m\pi}{L}\right)^2 + K_\phi\right] = M_{yy}(-A)\left(\frac{m\pi}{L}\right)^2 \tag{5}$$

The condition for existence of a non-zero- solution (A, B) gives

$$\left[GJ\left(\frac{m\pi}{L}\right)^2 + K_\phi\right]\left[EI_{zz}\left(\frac{m\pi}{L}\right)^4 + K_y\right] = M_{yy}^2\left(\frac{m\pi}{L}\right)^4 \tag{6}$$

The critical value of M_{yy}, for lateral buckling of the central pair, is determined by the lowest M_{yy} with respect to the integer m, and the buckling mode is determined by the associated integer m^*, at which the lowest M_{yy} is obtained, and the associated ratio A/B. In particular, if the surrounding elastic medium is absent and then $K_y = 0$ and $K_\phi = 0$, the lowest value of M_{yy} is $\frac{\pi}{L}\sqrt{GJEI_{zz}}$ with $m^* = 1$ [31].

The critical value of bending, given in terms of the ratio of the flagellum length to the radius of curvature of the bent flagellum ($Lw_0''(x)$), and the associated buckling mode, given in terms of the ratio of the buckling half-wavelength to the height of the central pair, are shown in Figs. 3 and 4, respectively, as a function of the length L of the flagellum. Here, it is stated that the (lowest) critical value for lateral buckling is associated with discontinuous mode-number (integer) m when the length L increases. This is responsible for the non-smoothness of the curves given in these figures for smaller lengths. This phenomenon is common in elastic buckling problems [31,32].

First, it is seen from Fig. 3 that for sufficiently long flagella (say, $L > 50H = 3$ μm), the critical value of the ratio $(\frac{M_{yy}L}{EI_{yy}})$ is directly proportional to L/H, which implies that the critical value of the moment M_{yy}, or the critical value of the radius of curvature of the bent flagellum $w_0''(x) = \frac{M_{yy}}{EI_{yy}}$, is independent of the length L. It should be stated that this conclusion essentially lies on the presence of the surrounding elastic medium. In fact, as stated above, in the absence of the surrounding elastic medium ($K_y = 0$ and $K_\phi = 0$), the critical value of M_{yy} for lateral buckling is inversely proportional to the length L. This can also be seen from the curve for $E_0 = 10^3$ Pa in Fig. 3(a), where the surrounding medium is extremely weak and, as a result, the critical value of $(\frac{M_{yy}L}{EI_{yy}})$ is almost independent of the length L within the range $L/H < 50$.

Another conclusion drawn from Fig. 3 is that the critical value for lateral buckling of the central pair is sensitive to the parameters defining the surrounding medium, but less sensitive to the shear modulus G of microtubules. Indeed, comparing Fig. 3(a) and (b) with Fig. 3(c) and (d) indicates that an increase of shear modulus G from $10^{-5}E$ to $10^{-3}E$ does not substantially change the critical value for lateral buckling. For example, for $E_0 = 10^5$ Pa and $K_y = 0.01E_0$, it is seen from Fig. 3(a) and (c) that the critical radius of curvature is 50 μm for $G = 10^{-5}E$, and 30 μm for $G = 10^{-3}E$. For $E_0 = 10^4$ Pa and $K_y = E_0$, it is seen from Fig. 3(b) and (d) that the critical radius of curvature is 15 μm for $G = 10^{-5}E$, and 12 μm for $G = 10^{-3}E$.

As one major conclusion for the buckling wavelength, it is seen from Fig. 4 that for sufficiently long flagella (say, $L > 200H = 12$ μm), the wavelength of the buckling mode is insensitive to the length L. It should be stressed that this conclusion essentially lies on the presence of the surrounding elastic medium. In fact, as stated above, in the absence

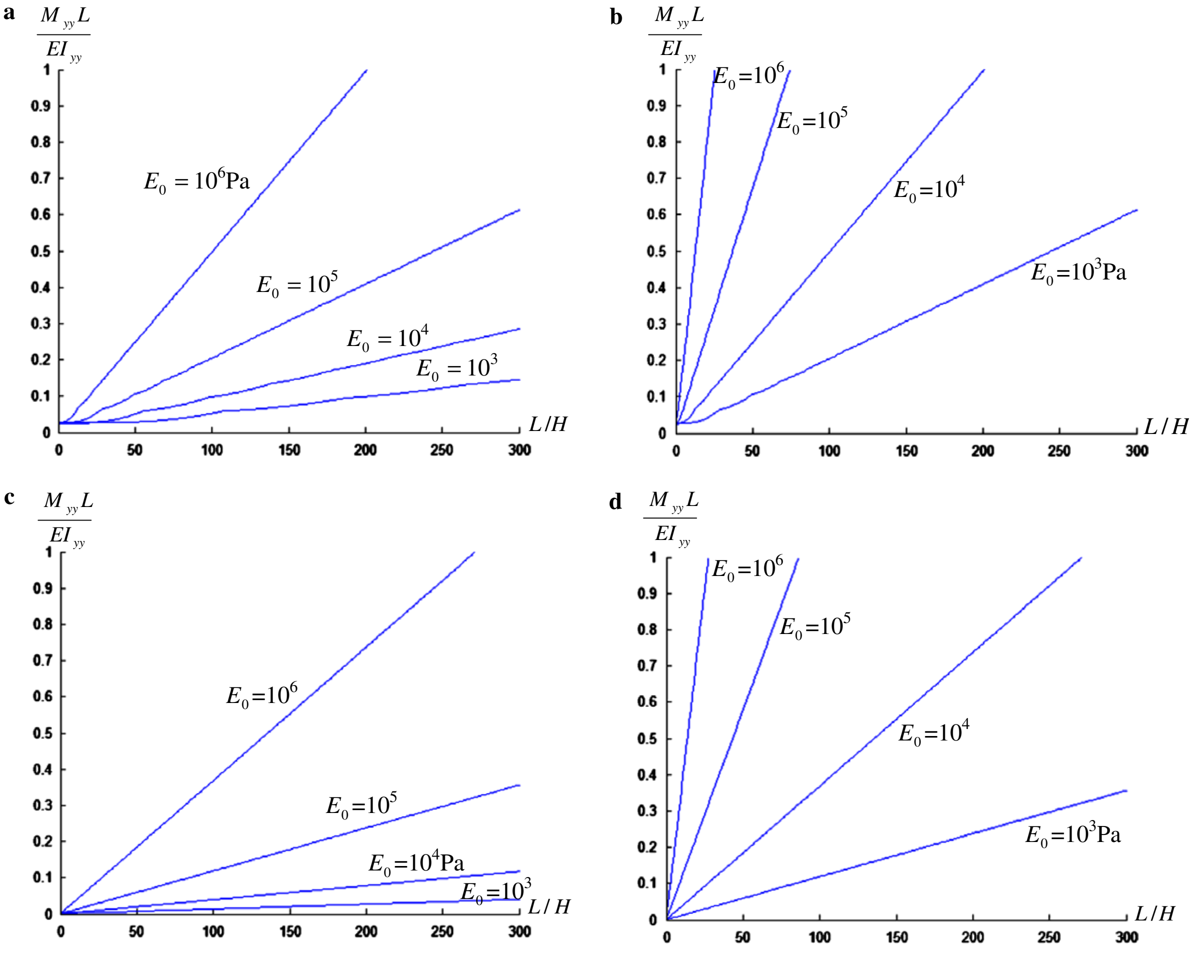

Fig. 3. Critical value for lateral buckling of the central pair under moment M_{yy} when (a) $G/E = 10^{-3}$ and $K_y = 0.01E_0$, (b) $G/E = 10^{-3}$ and $K_y = E_0$, (c) $G/E = 10^{-5}$ and $K_y = 0.01E_0$, (d) $G/E = 10^{-5}$ and $K_y = E_0$, where $\frac{M_{yy}L}{EI_{yy}}$ represents the ratio of the flagellum length to the radius of curvature of the bent flagellum.

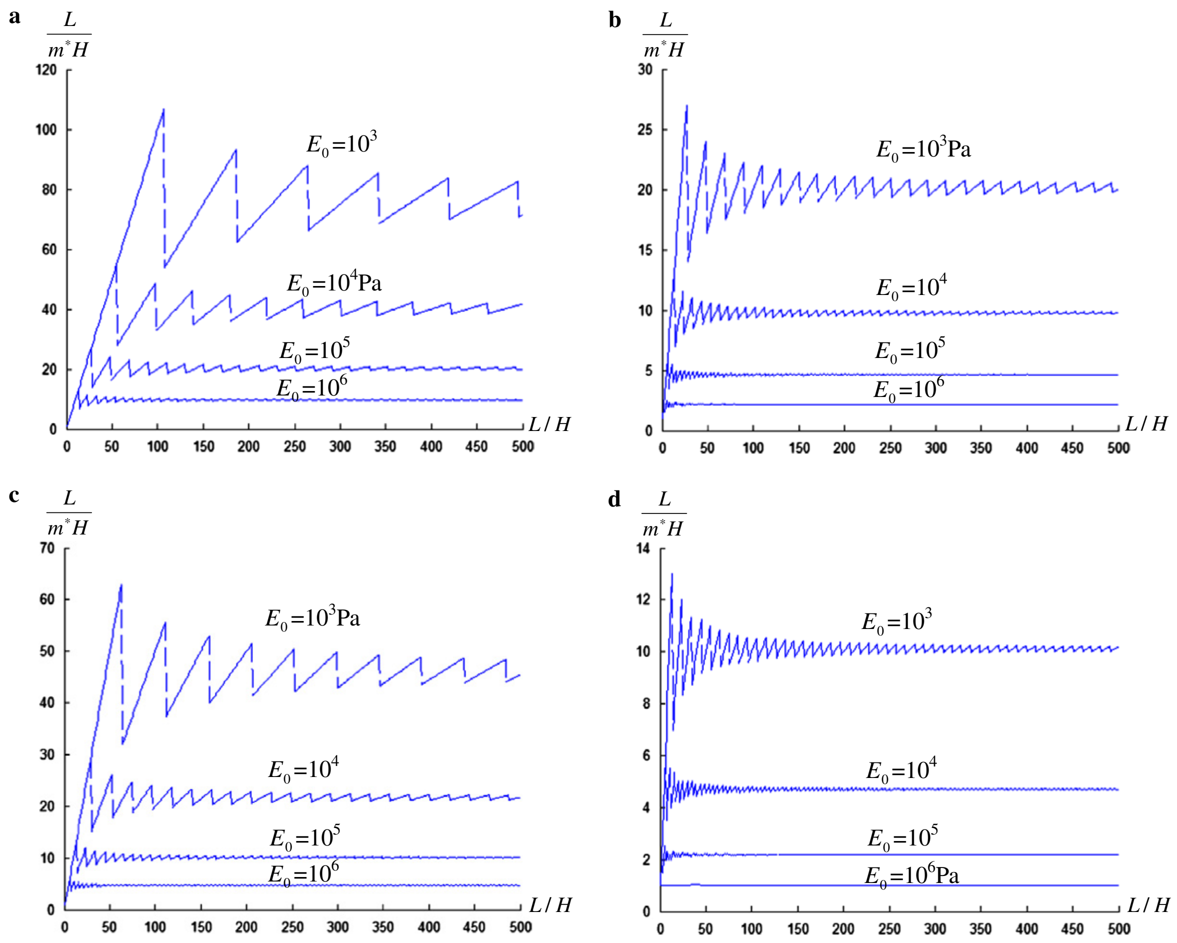

Fig. 4. The ratio of the buckling half-wavelength to the height H of the central pair for (a) $G/E = 10^{-3}$ and $K_y = 0.01E_0$, (b) $G/E = 10^{-3}$ and $K_y = E_0$, (c) $G/E = 10^{-5}$ and $K_y = 0.01E_0$, (d) $G/E = 10^{-5}$ and $K_y = E_0$.

of the surrounding elastic medium ($K_y = 0$ and $K_\phi = 0$), the half-wave number $m^* = 1$, and thus the half-wavelength of the buckling mode is equal to the flagellum length L. This can also be seen from the curve for $E_0 = 10^3$ Pa in Fig. 4(a), where the surrounding medium is extremely weak and, as a result, the half-wavelength $L/(m^*H)$ linearly increases with the length L within the range $L/H < 100$.

The wavelength of buckling mode for sufficiently long flagella can be estimated from Fig. 4. In particular, the buckling wavelength is sensitive to the parameters defining the surrounding medium, but less sensitive to the shear modulus G of microtubules. For example, when $E_0 = 10^3$ Pa and $K_y = E_0$, it is seen from Fig. 4(b) and (d) that the buckling wavelength is 1.2 μm for $G = 10^{-5}E$, and 2.4 μm for $G = 10^{-3}E$. On the other hand, for $E_0 = 10^4$ Pa and $K_y = 0.01E_0$, it is seen from Fig. 4(a) and (c) that the wavelength is 2.4 μm for $G = 10^{-5}E$ and 4.8 μm for $G = 10^{-3}E$. We noticed that these predicted wavelengths are comparable to related wavelengths (7–10 μ) observed previously [21–28].

In concluding our discussion, it should be stated that the present model is subjected to several limitations. First, the buckling analysis conducted in the paper is limited to static pure bending, although actual bending of flagella is always dynamic in nature and characterized by time-dependent and spacially non-uniform bending moment. Next, the present analysis is restricted to linearized small deflections of the flagellum and small rotations of the central pair. The dynamic and geometrically nonlinear effects on bending-driven torsional buckling of the central pair constitute a few interesting topics for further research.

Conclusions

A thin-walled elastic beam model is suggested to study why the central pair microtubules of eukaryotic flagella twists under bending. The results show that torsion of the central pair will occur inevitably, as a result of bending-driven lateral buckling of the central pair, especially when the flagellum is bent in the plane of the central pair's cross-section of the maximum bending rigidity. In this case, the critical curvature of bent flagellum for lateral buckling of the central pair is reasonably small and falls within a range of practical significance for flagellar motility. In particular, for a wide range of estimated parameters, the wavelengths of the buckling mode predicted by the present model are about a few microns and comparable to some known related experimental data. It is believed that the present paper identifies an important driving force for bending-driven torsion of the central pair, which has apparently not been uncovered in all previous related researches.

Acknowledgment

The financial support of the Natural Science and Engineering Research Council of Canada (NSERC) is gratefully acknowledged.

References

[1] R. Cotterill, Biophysics—An Introduction, John Wiley, New York, 2002.
[2] D. Boal, Mechanics of the Cell, Cambridge University Press, Cambridge, 2002.
[3] F.D. Warner, P. Satir, The substructures of ciliary microtubules, J. Cell Sci. 12 (1973) 313–326.
[4] J. Lighthill, Flagellar hydrodynamcis, SIAM Review 18 (1976) 161–226.
[5] I.R. Gibbons, Cilia and flagella of eukaryotes, J. Cell Biol. 91 (1981) 107–124.
[6] K.E. Machin, Wave propagation along flagella, J. Exp. Biol. 35 (1958) 796.
[7] C.J. Brokaw, Bend propagation along flagella, Nature 209 (1966) 161.
[8] C.J. Brokaw, Bending-wave propagation by microtubules and flagella, Math. Biosci. 90 (1988) 247–263.
[9] J.E. Schoutens, Predictions of elastic properties of sperm flagella, J. Theor. Biol. 171 (1994) 163.
[10] G.G. Vernon, D.M. Woolley, Microtubule displacements at the tips of living flagella, Cell Motil. Cytoskel. 52 (2002) 151.
[11] C.B. Lindemann, Structural–functional relationships of the dynein, spokes, and central-pair projections predicted from an analysis of the forces acting within a flagellum, Biophys. J. 84 (2003) 4115.
[12] J.E. Schoutens, A model describing bending in flagella, J. Biol. Phys. 30 (2004) 97.
[13] C. Cibert, J.V. Heck, Geometry drives the deviated-bending of the bi-tubular structure of the 9 + 2 axoneme in the flagellum, Cell Motil. Cytoskel. 59 (2004) 153.
[14] J. Gray, G.J. Hancock, The propulsion of sea-urchin spermatozoa, J. Exp. Biol. 32 (1955) 802.
[15] C. Brennen, H. Winer, Fluid mechanics of propulsion by cilia and flagella, Annual Review. Fluid. Mech. 9 (1977) 339.
[16] C.H. Wiggins, D. Riveline, A. Ott, R.E. Goldstein, Trapping and wiggling: elastohydrodynamics of driven microfilaments, Biophys. J. 74 (1998) 1043.
[17] R.H. Dillon, L.J. Fauci, An intergrative model of internal axoneme mechanics and external fluid dynamics in ciliary beating, J. Theor. Biol. 207 (2000) 415.
[18] C.J. Brokaw, Simulating the effects of fluid viscosity on the behavior of sperm flagella, Math. Method. Appl. Sci. 24 (2001) 1351.
[19] M. Kim, T.R. Powers, Hydrodynamic interaction between rotating helices, Phys. Rev. E 69 (2004) 061910.
[20] M. Manghi, X. Schlaberger, R.R. Netz, Propulsion with rotating elastic nanorods, Phys. Rev. Lett. 96 (2006) 068101.
[21] C.K. Omoto, C. Kung, The pair of central tubules rotates during ciliary beat in *Paramecium*, Nature 279 (1979) 534.
[22] C.K. Omoto, G.B. Witman, Functionally significant central-pair rotation in a primitive eukaryotic flagellum, Nature 290 (1981) 708.
[23] D.M. Woolley, G.G. Vernon, Alternative torsions in a living "9 + 2" flagellum, Proc. R. Soc. Lond. B 266 (1999) 1271.
[24] C.K. Omoto, Rotation of the central pair microtubules in eukaryotic flagella, Mol. Biol. Cell 10 (1999) 1–4.
[25] C. Cibert, Axonemal activity relative to the 2D/3D-waveform conversion of the flagellum, Cell Motil. Cytoskel. 51 (2002) 89–111.
[26] D.R. Mitchell, Orientation of the central pair complex during flagellar bend formation in *Chlamydomonas*, Cell Motil. Cytoskel. 56 (2003) 120.
[27] M.J. Wargo, E.F. Smith, Asymmetry of the central apparatus defines the location of active microtubule sliding in flagella, Proc. Natl. Acad. Sci. USA 100 (2003) 137.
[28] D.R. Mitchell, M. Nakatsugawa, Bend propagation drives central pair rotation in *Chlamydomonas reinhardtii* flagella, J. Cell Biol. 166 (2004) 709–715.
[29] K.A. Wemmer, W.F. Marshall, Flagellar motility: all pull together, Curr. Biol. 14 (2004) R992.
[30] R. Yokoyama, E.O. Toole, S. Ghosh, D.R. Mitchell, Regulation of flagellar dynein activity by a central pair kinesin, Proc. Natl. Acad. Sci. USA 101 (2004) 17398.
[31] S.O. Timoshenko, J.M. Gere, Theory of Elastic Stability, McGraw-Hill, New York, 1961.
[32] A. Chajes, Principles of Structural Stability Theory, Prentice-Hall, Englewood Cliffs, NJ, 1974.
[33] R.L. Serrette, T. Pekoz, Distorsional buckling of thin-walled beams/panels, J. Struct. Eng. 121 (1995) 757.
[34] J.G. Teng, J. Yao, Y. Zhao, Distorsional buckling of channel beam-columns, Thin Wall. Struct. 41 (2003) 595.
[35] J. Howard, Mechanics of Motor Proteins and the Cytoskeleton, Sinauer Associates, Inc., Sunderland, 2001.
[36] F. Gittes, B. Mickey, J. Nettleton, J. Howard, Flexural rigidity of microtubules and actin filaments measured from thermal fluctuation in shape, J. Cell Biol. 120 (1995) 923–934.
[37] Y.M. Sirenko, M.A. Stroscio, K.W. Kim, Elastic vibration of microtubules in a fluid, Phys. Rev. E 53 (1996) 1003–1010.
[38] T. Takasone, S. Juodkazis, Y. Kawagishi, A. Yamaguchi, S. Matsuo, H. Sakakibara, H. Nakayama, H. Misawa, Flexural rigidity of a single microtubule, Japaness J. Appl. Phys. 41 (2002) 3015–3019.
[39] P.J. Pablo, L.A.T. Schaap, F.C. Mackintosh, C.F. Schmit, Deformation and collapse of microtubules on the nanometer scale, Phys. Rev. Lett. 91 (2003) 098101.
[40] C. Li, C.Q. Ru, A. Mioduchowski, Length dependence of flexural rigidity as a result of anisotropic elastic properties of microtubules, Biochem. Biophys. Res. Commun. 349 (2006) 1145–1150.
[41] R.D. Cook, W.C. Young, Advanced Mechanics of Materials, second ed., Prentice Hall, New Jersey, 1999.
[42] W.B. Bickford, Advanced Mechanics of Materials, Addison-Wesley. Menlo Park, CA, 1998.
[43] A. Kis, S. Kasas, B. Babic, A.J. Kulik, W. Benoît, G.A.D. Briggs, C. Schönenberger, S. Catsicas, L. Forró, Nanomechanics of microtubules, Phys. Rev. Lett. 89 (2002) 248101.
[44] J.A. Tuszynski, T. Luchko, S. Portet, J.M. Dixon, Anisotropic elastic properties of microtubules, Eur. Phys. J. E17 (2005) 29–35.
[45] G. Bao, S. Suresh, Cell and molecular mechanics of biological materials, Nature Materials 2 (2003) 715–725.
[46] J. Yoon, C.Q. Ru, A. Mioduchowski, Vibration of an embedded multiwall carbon nanotube, Compos. Sci. Technol. 63 (2003) 1533–1542.
[47] C.Q. Ru, Elastic models for carbon nanotubes, in: H.S. Nalwa (Ed.), Encyclopedia of Nanoscience and Nanotechnology, vol. 2, American Scientific Publishers, 2004, pp. 731–744.